European Journal of Medicinal Chemistry 135 (2017) 49–59

Contents lists available at ScienceDirect

European Journal of Medicinal Chemistry

journal homepage: http://www.elsevier.com/locate/ejmech

Research paper

# First example of peptides targeting the dimer interface of *Leishmania infantum* trypanothione reductase with potent *in vitro* antileishmanial activity[#]

Marta Ruiz-Santaquiteria [a], Pedro A. Sánchez-Murcia [b], Miguel A. Toro [c], Héctor de Lucio [c], Kilian Jesús Gutiérrez [c], Sonia de Castro [a], Filipa A.C. Carneiro [a], Federico Gago [b], Antonio Jiménez-Ruiz [c], María-José Camarasa [a], Sonsoles Velázquez [a, *]

[a] *Instituto de Química Médica (IQM-CSIC), E-28006 Madrid, Spain*
[b] *Área de Farmacología, Departamento de Ciencias Biomédicas, Unidad Asociada al IQM-CSIC, Universidad de Alcalá, E-28805 Alcalá de Henares, Madrid, Spain*
[c] *Departamento de Biología de Sistemas, Universidad de Alcalá, E-28805 Alcalá de Henares, Madrid, Spain*

ARTICLE INFO

*Article history:*
Received 17 February 2017
Received in revised form
30 March 2017
Accepted 11 April 2017
Available online 13 April 2017

[#]Dedicated to Professor Jan Balzarini on the occasion of his retirement

*Keywords:*
Peptides
Helix stabilization
Protein-protein interactions
Trypanothione reductase
*Leishmania infantum*
Cell-penetrating peptides

ABSTRACT

A series of 9-mer and 13-mer amide-bridged cyclic peptides derived from the linear prototype Ac-PKIIQSVGIS-Nle-K-Nle-$NH_2$ (Toro et al. *ChemBioChem* **2013**) has been designed and synthesized by introduction of the lactam between amino acid side chains that are separated by one helical turn (*i*, *i*+*4*). All of these compounds were tested *in vitro* as both dimerization and enzyme inhibitors of *Leishmania infantum* trypanothione reductase (Li-TryR). Three of the 13-mer cyclic peptide derivatives (**3, 4** and **6**) inhibited the oxidoreductase activity of Li-TryR in the low micromolar range and they also disrupted enzyme dimerization. Cyclic analogues **3** and **4** were more resistant to proteases than was the linear prototype. Furthermore, the most potent TryR inhibitors in the linear and cyclic series displayed potent *in vitro* activity against *Leishmania infantum* upon conjugation with cationic cell-penetrating peptides. To date, these conjugated peptides can be considered the first example of TryR dimerization inhibitors that are active in cell culture.


## 1. Introduction

*Leishmania* parasites are the causative agents of leishmaniasis, one of the World Health Organization's 16 neglected tropical diseases and endemic in more than 80 countries worldwide. One of the most serious clinical forms of this disease is visceral leishmaniasis (VL), caused by *L. donovani*, *L. infantum and L. chagasi*, which is invariably fatal if left untreated. VL kills more than 20000 people every year and over 310 million people are considered at risk of infection [1]. Furthermore, reported cases of *Leishmania* and HIV co-infection in many endemic countries continue to be of great concern. Current drugs are highly toxic, resistance is common, and patient compliance is low as the medicines are costly and treatments are long [2–4]. Thus, there is an urgent need to identify and develop new and more efficient nontoxic and innovative drugs to fight this infection.

Trypanothione reductase (TryR) of trypanosomatids is a validated drug target as this is a crucial enzyme in their defense against oxidative stress and is absent in humans [5]. Most, if not all, the efforts made by the scientific community to inhibit TryR have relied on the design of molecules directed towards the active site, some of which have turned out to be lethal to whole parasites *in vitro* [6–8].

*Abbreviations:* CPP, cell-penetrating peptide; DSSP, define secondary structure of proteins algorithm; ELISA, Enzyme-Linked ImmunoSorbent Assay; $IC_{50}$, inhibitory concentration 50; Li-TryR, *Leishmania infantum* trypanothione reductase; $LC_{50}$, lethal concentration 50; MD, molecular dynamics; Mmt, monomethoxytrityl; Phipr, phenylisopropyl; PyBOP, (benzotriazol-1-yloxy)tripyrrolidino phosphonium hexafluorophosphate; PPIs, protein-protein interaction inhibitors; PI, propidium iodide; SPPS, solid phase peptide synthesis; TFE, trifluorethanol; VL, visceral leishmaniasis.

* Corresponding author. Instituto de Química Médica (CSIC), C/ Juan de la Cierva 3 E-28006 Madrid, Spain.
*E-mail address:* iqmsv29@iqm.csic.es (S. Velázquez).

http://dx.doi.org/10.1016/j.ejmech.2017.04.020

Considering that the biologically functional form of TryR is a homodimer, we have recently reported [9] an unexploited inhibition strategy directed at disrupting the dimer interface of the enzyme by means of protein-protein interaction inhibitors (PPIs). Previously, using a combination of molecular modeling and site-directed mutagenesis studies, we identified and validated E436 as a key amino acid ("hot spot") for the structural stability and function of the dimer. On the basis of these results and as a "proof of concept" of this novel approach, we designed and tested a small library of linear peptides representing rational variations of the α-helix, spanning residues P435 to M447, that contains the crucial E436 of *Leishmania infantum* TryR (Li-TryR). Among the synthesized peptides, the 13-mer peptide Ac-PKIIQSVGIS-Nle-K-Nle-$NH_2$, containing Lys in place of Glu at position 2, outperformed the original sequence (Ac-PEIIQSVGIS-Nle-K-Nle-$NH_2$, compound **P1**) in inhibiting both Li-TryR dimerization and oxidoreductase activity in a sequence-specific manner [9]. These findings were rationalized by results from molecular dynamics (MD) simulations that highlighted a strong electrostatic interaction between the Lys at position 2 of the peptide and E436 in the Li-TryR monomer, a key residue for enzyme stability. Furthermore, we identified the 9-mer peptide Ac-PKIIQSVGI-$NH_2$ as the shortest C-terminally truncated peptide that was able to inhibit Li-TryR [9]. Therefore, these peptides emerged as promising Li-TryR dimerization inhibitors in the micromolar range [9]. Nonetheless, these linear prototypes derived from the 435–447 α-helix were inactive against *L. infantum* axenic amastigotes and promastigotes, most likely because the theoretically predicted low propensity to form an α-helix in solution prevents crossing of cell membranes. For this reason, we recently explored strategies for stabilizing the helical content of the original peptide sequence **P1** in solution by side chain-to-side chain cyclization through carbon-carbon or amide bonds [10]. The use of both lactam bridges [11–14] and short hydrocarbon chains [15,16] as staples proved to be successful to enhance and maximize helicity as well as to limit degradation by proteases [17–19]. Our germinal results indicated that the nature of the introduced linker had a deep impact on the potency as Li-TryR dimerization inhibitors of **P1** derivatives of general formula Ac-PEIXQSVXIS-Nle-K-Nle, where X indicates the position of the cyclizing residues. Notably, the dicarba analogs of **P1** had no measurable activity but the lactam derivatives not only retained the inhibitory potency found in their linear counterparts but they were also more resistant to proteolytic degradation [10].

In the work reported herein, the overall aim was to increase the proteolytic stability and to improve the *in vitro* leishmanicidal activity of previously described Li-TryR-derived linear peptides that were active as TryR dimerization inhibitors [9]. To achieve this goal, we first synthesized and characterized a series of amide-bridged cyclic analogues, derived from the most potent 13-mer and 9-mer linear prototypes identified so far (compounds **1** and **2**, Fig. 1). Macrolactam constraints were introduced between amino acid side-chains that are separated by one helical turn (*i, i+4*) (compounds **3**–**8**, Fig. 1). Of these new amide-bridged derivatives, **3**, **4** and **6** inhibited the oxidoreductase activity of Li-TryR in the low micromolar range and were also active in disrupting enzyme dimerization. The conformational constraints introduced improved the proteolytic stability of these derivatives against proteinase K, a broad-spectrum serine-protease. On the other hand, conjugation with cationic cell-penetrating peptides (CPP) of the linear and cyclic peptides that were most active in the enzymatic assays was also explored. Interestingly, these conjugates displayed potent *in vitro* activity against *Leishmania infantum* parasites. To date, and to the best of our knowledge, these compounds represent the first reported TryR dimerization inhibitors that are active in cell culture.

## 2. Results and discussion

### 2.1. Design and chemical synthesis

We explored several positions for covalent amide closure in both 13-mer and 9-mer peptides, all of them placed on the face of the α-helix opposite to that used for binding to the Li-TryR monomer (Fig. 1). The sequences of the target cyclic peptides (**3**–**8**) are depicted in Fig. 1.

The synthesis of **3**–**8** was performed manually following standard solid-phase peptide synthesis (SPPS) protocols using a Rink amide MBHA polystyrene resin and *N*-Fmoc/$^t$Bu chemistry. The peptides were isolated both acetylated at the *N*-terminus and as carboxamides at the *C*-terminal end. A low load of resin (0.38 mmoL/g) was used to minimize oligomer formation during the side chain-to-side chain cyclization.

The synthesis of 13-mers **3**–**6** is depicted in Scheme 1. For the preparation of lactam **3**, **4** and **6**, we used commercially available Glu and Lys residues with the side-chains protected as allyl esters and allyloxycarbonyl groups suitable for orthogonal deprotection prior to on-resin cyclization (**Method a**, Scheme 1). After Fmoc deprotection of the resin under standard piperidine conditions, the first amino acid was introduced in the presence of HCTU as the coupling reagent and DIEA as the base at room temperature for 2 h. The coupling of the following amino acids was carried out under microwave irradiation at 40° C in the presence of HCTU/DIEA (3 × 10 min). Once the elongation was completed, the Fmoc-group of the *N*-terminus of the peptides was deprotected and acetylated. Next, the allyl groups were selectively removed with $Pd(PPh_3)_4$ and $PhSiH_3$ as an allyl scavenger, and then, the lactam bridge was formed using PyBOP and DIEA in NMP as solvent. The lactam-forming reaction was completed at room temperature in 1 h. Finally, the cyclic peptides were cleaved from the resin under standard conditions. The 9-mer cyclic analogues **7** and **8** were similarly prepared (see Experimental). The corresponding 13-mer and 9-mer linear precursors **14, 15, 17**–**19** (Table S1, see Supplementary material) were also synthesized by cycles of Fmoc-deprotection and coupling, acetylation, removal of the allyl groups and final cleavage from the resin.

Our initial attempts to synthesize **5** using a similar Fmoc/allyl/tBu strategy consistently failed due to the high propensity of the unhindered allyl ester-protected glutamate adjacent to a Gly residue to undergo base-induced glutarimide formation [20]. For preventing this side–reaction, the sterically demanding mild acid-labile protecting groups monomethoxytrityl (Mmt) and phenyl-isopropyl (Phipr) groups were used for the protection of the bridging Lys and Glu residues, respectively (**Method b**, Scheme 1). Thus, after elongation of the first seven residues, the Glu and Lys side-chain groups were deprotected with dilute TFA (1%). Cyclization was then carried out with PyBOP as the coupling reagent. Upon subsequent peptide chain elongation, the *N*-terminus of the peptide was acetylated and cleaved from the resin under standard conditions to give the desired 13-mer cyclic compound **5**. The corresponding linear precursor **16** (Table S1, see Supplementary material) was also prepared after completing the elongation, acetylation and standard TFA cleavage leading to the simultaneous deprotection of the side-chains of Glu(Phipr) and Lys(Mmt) residues.

Every cyclic peptide and linear precursor synthesized in this work was characterized by analytical HPLC and ESI-MS after purification on a Biotage Isolera (linear analogues) or by semi-preparative HPLC (cyclic analogues). The sequences, HPLC purity and global yields of the target cyclic peptides and linear precursors are shown in Table S1 (see Supplementary material).

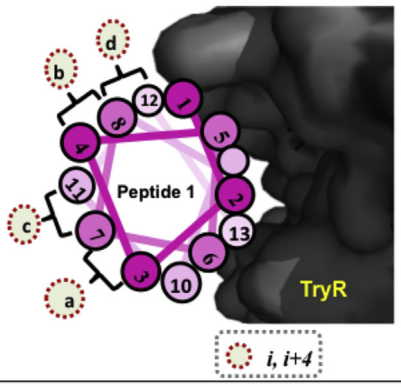


| Peptide number (cyclization position)[a] | Peptide sequence | | | | | | | | | | | | |
|---|---|---|---|---|---|---|---|---|---|---|---|---|---|
| | 1 | 2 | 3 | 4 | 5 | 6 | 7 | 8 | 9 | 10 | 11 | 12 | 13 |
| 1 | P | K | I | I | Q | S | V | G | I | S | $N_L$ | K | $N_L$ |
| 2 | P | K | I | I | Q | S | V | G | I | | | | |
| 3 (a) | P | K | E | I | Q | S | K | G | I | S | $N_L$ | K | $N_L$ |
| | | | CO–NH | | | | | | | | | | |
| 4 (b) | P | K | I | E | Q | S | V | K | I | S | $N_L$ | K | $N_L$ |
| | | | | CO–NH | | | | | | | | | |
| 5 (c) | P | K | I | I | Q | S | E | G | I | S | K | K | $N_L$ |
| | | | | | | | CO–NH | | | | | | |
| 6 (d) | P | K | I | I | Q | S | V | E | I | S | $N_L$ | K | $N_L$ |
| | | | | | | | | CO–NH | | | | | |
| 7 (a) | P | K | E | I | Q | S | K | G | I | | | | |
| | | | CO–NH | | | | | | | | | | |
| 8 (b) | P | K | I | E | Q | S | V | K | I | | | | |
| | | | | CO–NH | | | | | | | | | |

[a] Cyclization positions a-d according to Figure 1
$N_L$ = norleucine

**Fig. 1.** Sequences and cyclization positions (on the side of the α-helix side that is thought not to interact directly with Li-TryR) of the designed lactam peptides synthesized in this work.

### 2.2. Structural characterization

The helical content of peptides **3**–**8** was studied by means of circular dichroism (CD) spectroscopy and molecular modeling. The percentage of helicity for each cyclic peptide and linear precursor was calculated according to its molar ellipticity at 222 nm and the number of amino acids using the equation of Baldwin and col [21]. (see table in Fig. 2). To increase the aqueous solubility of the peptides the CD-UV spectra were acquired in the presence of the helix-promoting solvent 2,2,2-trifluoroethanol (TFE) [22,23].

In all cases, the introduction of the amide covalent closure promoted α-helical formation: whereas the linear prototypes **1** and **2**, as well as the linear 9-mer and 13-mer precursors **14**–**19**, exhibited a CD spectrum characteristic of unstructured peptides (data not shown), all the cyclic peptides **3**–**8** displayed the dual minima at 208 and 222 nm characteristic of an α-helix (Fig. 2). As expected due to their increased length, the lactam-bridged **3**–**6** 13-mers, irrespective of the position of cyclization, exhibited higher percentages of helicity compared to the linear prototype **1** (38–65% *vs* 16%) (Fig. 2A). In contrast, the two amide-bridged 9-mers **7** and **8** behaved differently (Fig. 2B) insofar as cyclization between positions 3 and 7 (**7**) was found to be less beneficial for helicity than cyclization between positions 4 and 8 (**8**).

To get some insight into the structural effects of introducing these amide bonds between positions 3,7 or 4,8 we ran unrestrained MD simulations of 9-mers **7** and **8** in explicit water. We found, in both cases, an increase in the percentages of α-helices in comparison to their linear counterpart **2**, in consonance with the experimental findings (Fig. 3). Nonetheless, in **7** only the five central residues (4–8) maintained the α-helical structure (Fig. 3A) whereas two complete helical turns covering the whole sequence were apparent in **8** during most of the simulation (Fig. 3B).

### 2.3. Biological activity

#### 2.3.1. Enzymatic assays and proteolytic stability

All the synthetized compounds (including intermediates **14**–**19**) were evaluated as Li-TryR inhibitors [24] (Table 1). The position of the linking residues in the peptide sequence of the amide-bridged cyclic 13-mers was found to be crucially important for their Li-TryR inhibitory activity. Thus, the $IC_{50}$ values of **3** and **4**, with a lactam bridge at positions 3, 7 and 4, 8, respectively, were similar to that of the linear prototype **1** whereas substantial drops in inhibitory potency were apparent for **5** and **6**, which are cyclized through positions 7 and 11 or 8 and 12, respectively. None of the two shorter cyclic 9-mers, **7** and **8**, displayed any activity but **19** (the linear

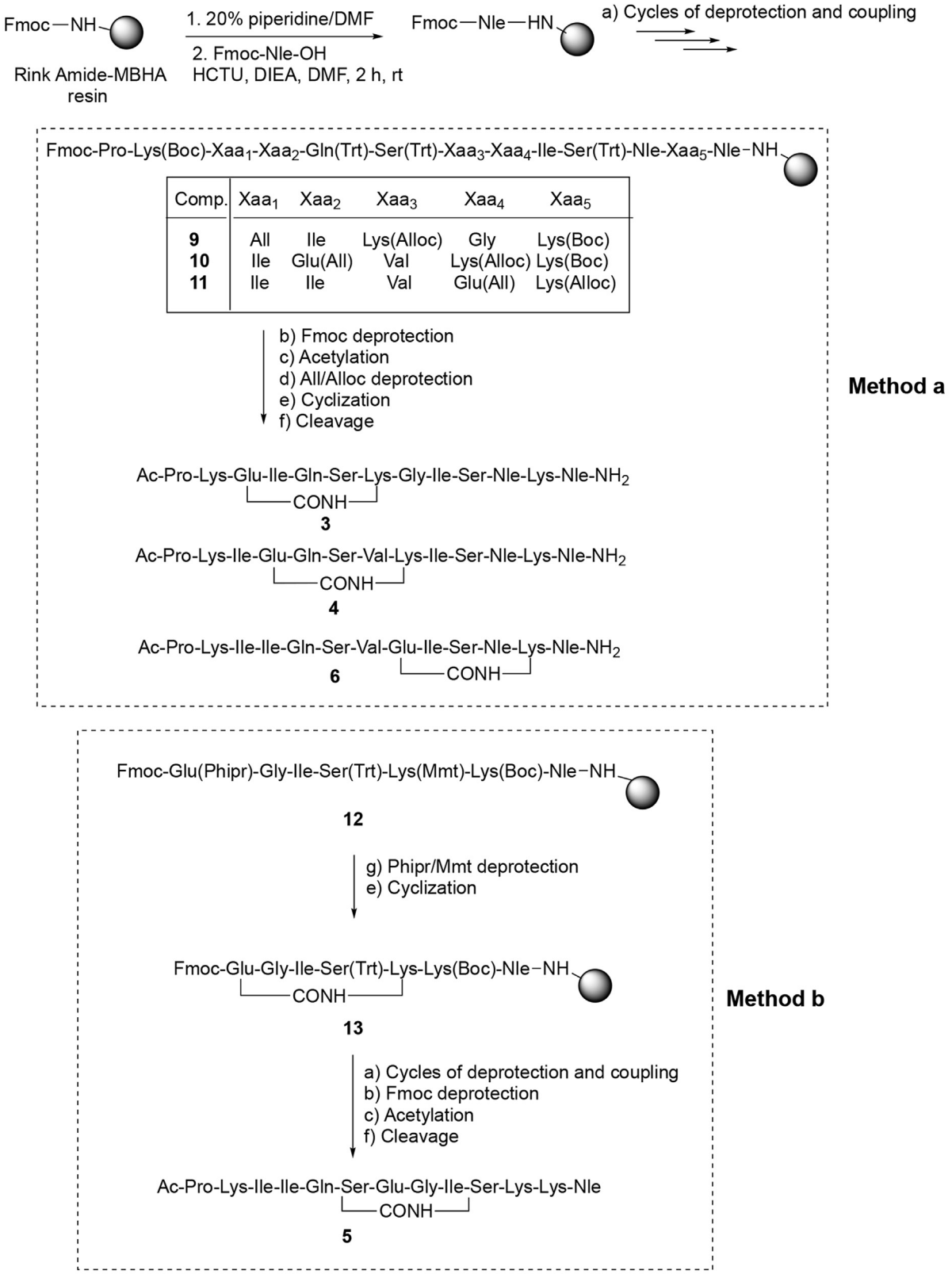


*Reagents and conditions*: (a) 20% piperidine, DMF, rt; Fmoc-AA-OH; HCTU, DIEA, DMF, MW, 3 x 10 min, 40 °C; (b) 20% piperidine, DMF, rt; (c) $Ac_2O$, DIEA, DMF, rt; (d) $Pd(PPh_3)_4$, $PhSiH_3$, DCM, rt; (e) PyBOP, DIEA, NMP, 1 h, rt; (f) TFA/TIPS/$H_2O$ (95:2.5:2.5), rt; (g) TFA/TIPS/DCM (1:2:97), rt.

**Scheme 1.** Synthesis of amide-bridged cyclic peptides **3, 4, 6** (**Method a**) and **5** (**Method b**).

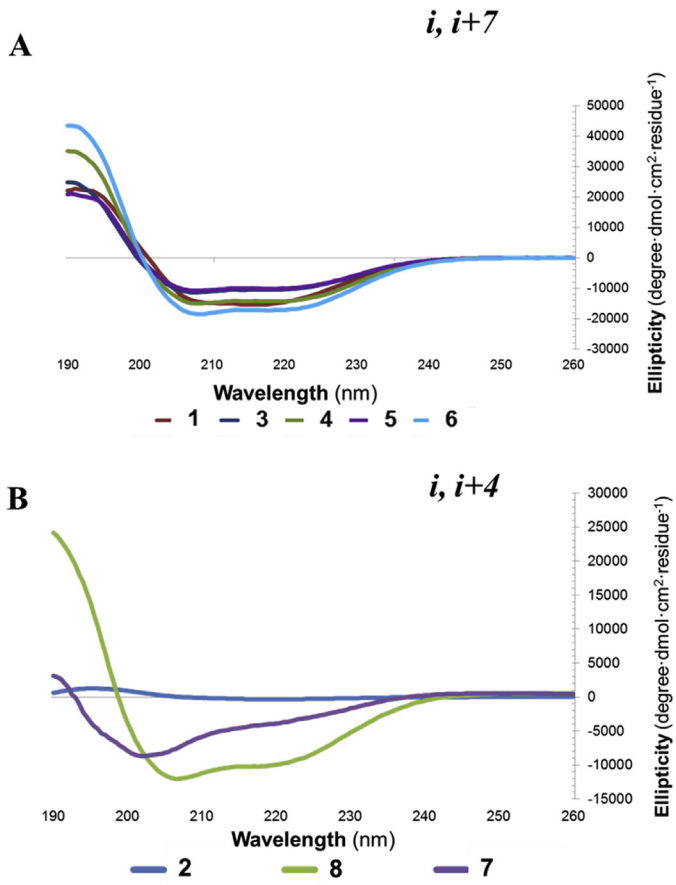


| | Peptides | *Helicity (%)* |
|---|---|---|
| *9-mer* | 2 (linear) | 1.5 |
| | 7 | 16 |
| | 8 | 45 |
| *13-mer* | 1 (linear) | 16 |
| | 3 | 40 |
| | 4 | 55 |
| | 5 | 38 |
| | 6 | 65 |

**Fig. 2.** (Left) Circular dichroism spectra of amide-bridged 13-mers **3**–**6** (A) and amide-bridged 9-mers **7** and **8** (B). Linear peptides **1** and **2** were used as controls. (Right) Experimentally determined helicities (%).

precursor of **8**) was found to be moderately active against the enzyme.

The next step was to explore whether the inhibitory activity detected in this assay was contingent on the disruption of the dimeric form of the enzyme, as originally intended [9]. In good agreement with our expectations, all the cyclic compounds found to be active in the enzymatic assay (**3**, **4** and **6**) were also shown to be Li-TryR dimerization disruptors in our ELISA assay (Table 1) [9].

Taken together, our data support the view that a minimal backbone flexibility is required to keep the inhibitory potency in the cyclic derivatives. Whereas side-chain cross-linking of amino acids at positions 3, 7 and 4, 8 of the linear 13-*mer* **1** (yielding **3** and **4**, respectively) does not reduce the activity, cross-linking of the same positions in the linear 9-*mer* **2** completely abolishes the activity in derivatives **7** and **8**. Furthermore, activity does not appear to depend on helix propensity as no clear differences are found between active and inactive peptides in their heat maps for secondary structure (Fig. 3 and Fig. S1, see Supplementary material). Interestingly, the MD simulations of 13-mer cyclic peptides suggest that the loss of activity in **5** (cross-linked at 7, 11) is likely due to its being locked in a rigid non-bioactive conformation (Fig. S1, top right), in contrast to **6** (cross-linked at 8, 12), which is active and maintains a structure like that of the also active **3** and **4** (cross-linked at 3, 7 and 4, 8, respectively) (Fig. S1, top and bottom left). Finally, although the last three residues in the linear 13-*mers* are not required for activity [9], this *C*-terminal region appears to be critical for inhibitory potency in the presence of a side-chain crosslink (peptides **3**, **4** and **6**) (Table 1).

To determine the influence of lactam-bridge stapling on proteolytic stability, we compared the susceptibilities of the linear prototype **1** and the most active lactam-containing analogues **3** and **4** to degradation by proteinase K, a promiscuous serine protease with broad substrate specificity. The half-lives of the lactam-bridged analogues **3** and **4** were 2- to 3-fold higher than that of the linear analogue **1** ($t_{1/2}$ values of 52 and 64 min *vs* 23 min, respectively).

### 2.3.2. Anti-leishmanial activity in cell culture

The linear and cyclic analogues were tested *in vitro* against *L. infantum* promastigotes and axenic amastigotes using edelfosine and miltefosine as positive controls. Since none of the newly synthetized compounds displayed any activity at 25 μM (maximum concentration assayed), we examined their ability to cross the plasma membrane. Fluorescence microscopy of promastigotes incubated with the fluoresceine–labeled peptide conjugates of (compounds **20** and **21**, Fig. S2, see Supplementary material) demonstrated the low ability of linear prototype **1** and the lactam-bridged analogue **3** to cross the cell membrane (data not shown).

In an attempt to increase cell permeability, both compounds were covalently linked to a CPP through their *N*-terminal or *C*-terminal regions [25–27]. Among the cationic CPPs, the widely used polyarginines ($R_9$) and Tat sequences were selected due to their recently reported low toxicity and efficient uptake by *Leishmania* parasites and macrophages [28,29]. Moreover, stabilized α-aminoisobutyric acid (Aib)-containing Arg-based peptides were also chosen [30]. It should be noted that CPP-based approaches have been rarely explored for infectious diseases such as leishmaniasis. The sequences of the target [CPP]-[peptide] conjugates

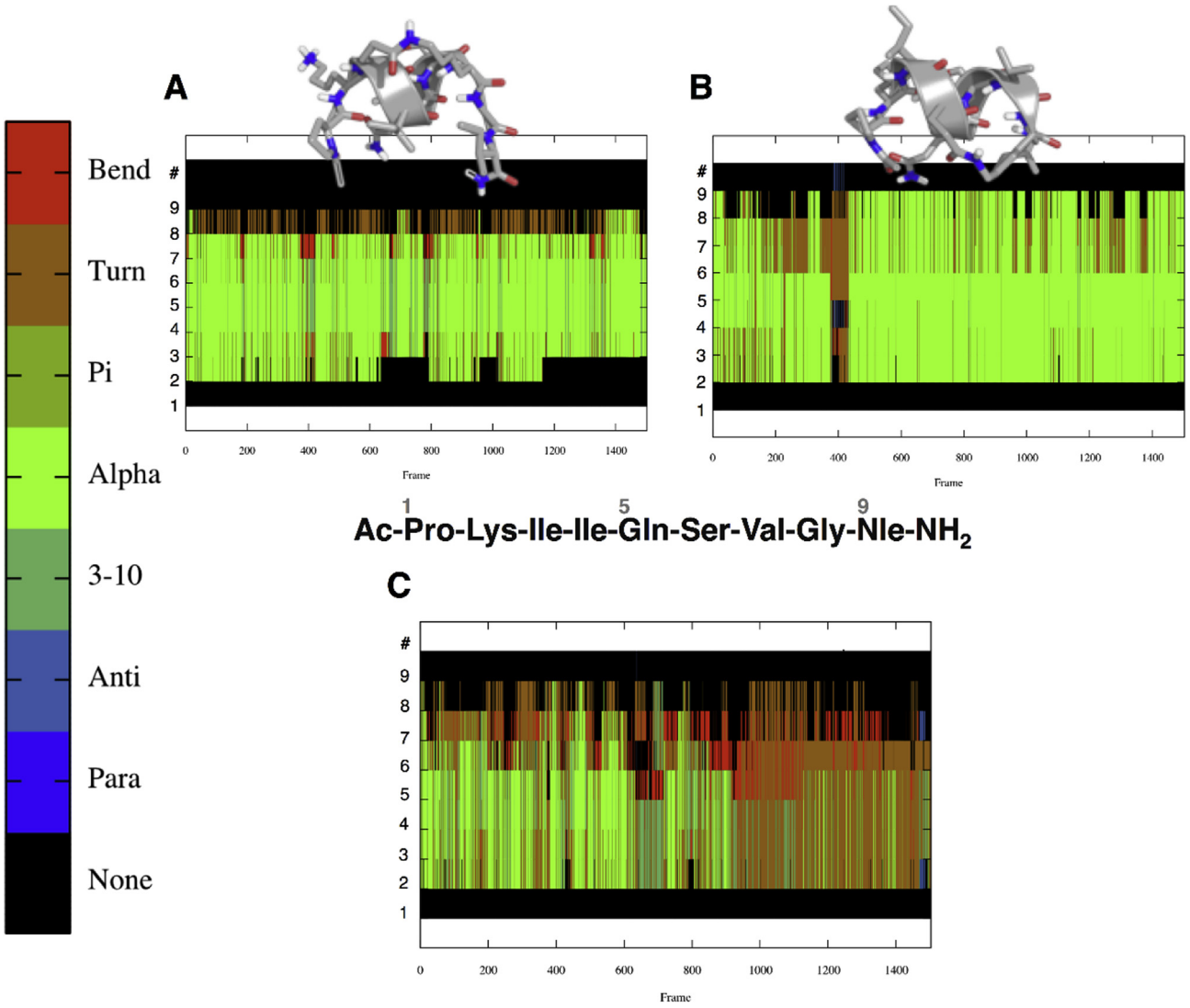


**Fig. 3.** Heat maps of secondary structure propensity per residue (#) of the cyclic 9-mers **7** (A) and **8** (B), and their linear counterpart **2** (C) over 150 ns(1500 snapshots) of unrestrained MD simulation in aqueous solution. A representative conformation of **7** and **8** from the respective most populated cluster is displayed on top of each heat map.

**Table 1**
$IC_{50}$ ± SEM values for linear and cyclic peptides **1**–**8** and **14**–**19** in the TryR oxidoreductase activity and Li-TryR monomer displacement assays.

| Peptide | $IC_{50}$ activity (μM)[a] | $IC_{50}$ dimerization (μM)[b] |
|---|---|---|
| **1** (linear 13-mer prototype) | 1.2 ± 0.2 | 13.5 ± 2.4 |
| **2** (linear 9-mer prototype) | 3.7 ± 0.3 | 20.8 ± 0.5 |
| **3** (3,7-lactam-bridged 13-mer) | 0.9 ± 0.1 | 9.9 ± 1.6 |
| **4** (4,8-lactam-bridged 13-mer) | 5.3 ± 0.8 | 14.4 ± 1.8 |
| **5** (7,11-lactam-bridged 13-mer) | >75 | >75 |
| **6** (8,12-lactam-bridged 13-mer) | 27.0 ± 3.2 | 12.1 ± 0.3 |
| **7** (3,7-lactam-bridged 9-mer) | >75 | >75 |
| **8** (4,8-lactam-bridged 9-mer) | >75 | >75 |
| **14** (linear precursor **3**) | >75 | – |
| **15** (linear precursor **4**) | >75 | – |
| **16** (linear precursor **5**) | >75 | – |
| **17** (linear precursor **6**) | >75 | – |
| **18** (linear precursor **7**) | >75 | – |
| **19** (linear precursor **8**) | 47.4 ± 11.6 | – |

[a] Enzymatic activity > 75 indicates that the $IC_{50}$ value is higher than 75 μM (maximum assayed). Results are representative of three independent experiments, each performed in triplicate.
[b] Dimer quantitation assay (ELISA) [9].

**22**–**26** are given in Table 2. Non-conjugated $R_9$ and Tat sequences (**27** and **28**), and an $R_9$-conjugated scrambled peptide (**29**) were also studied as controls.

As expected, linkage of a CPP to our TryR inhibitors facilitated passage through the plasma membrane and converted our peptide prototypes into leishmanicidal agents showing $LC_{50}$ values against amastigotes of the same order as those observed for miltefosine (Table 2). The activity of the conjugates against monocytic THP-1 cells might be caused by an undesired off-target effect on related human oxidoreductases that is currently being studied.

Our results indicate that the leishmanicidal activity of $R_9$- (**22** and **23**) and Tat-conjugated peptides (**24**) of linear prototype **1** is similar. Moreover, the potency of our conjugated prototype **1** is not dependent on the position of the $R_9$ sequence at either the N- or C-terminus of the peptide. The $R_9$-conjugated cyclic peptide (compound **25**) displayed an activity similar to that of the $R_9$-conjugated linear analogues. In addition, the $LC_{50}$ values obtained for **26** (the $(RR\text{-}Aib)_3$-conjugate of cyclic derivative **3**) in promastigotes, amastigotes and THP-1 cells are higher than those observed for the $R_9$ conjugate **25**, which suggests a lower cell-penetrating capacity of this CPP.

**Table 2**
$LC_{50}$[a] ± SEM values for the [CPPs]-[peptide] conjugates **22**–**26**, CPPs $R_9$ and Tat (**27** and **28**) and $R_9$-conjugated scrambled peptide **29** on *L. infantum* promatigotes, amastigotes and THP-1 cells.[b]

| Comp. | Sequence[c] | $LC_{50}$ (μM) Promastigotes | $LC_{50}$ (μM) Amastigotes | $LC_{50}$ (μM) THP-1 |
|---|---|---|---|---|
| **22** | RRRRRRRRR PKIIQSVGISN$_L$KN$_L$ | 4.6 ± 0.2 | 3.5 ± 0.9 | 1.7 ± 0.5 |
| **23** | PKIIQSVGISN$_L$KN$_L$ RRRRRRRRR | 4.4 ± 0.5 | 2.1 ± 1.0 | 0.8 ± 0.1 |
| **24** | GRKKRRQRRRPPQ PKIIQSVGISN$_L$KN$_L$ | 4.3 ± 0.4 | 1.5 ± 0.3 | 1.2 ± 0.4 |
| **25** | RRRRRRRRRPK-c[(CH$_2$)$_2$CONH(CH$_2$)$_4$]$^{3,7}$ [EIQSK]GISN$_L$KN$_L$ | 3.5 ± 0.4 | 2.8 ± 0.3 | 2.5 ± 0.8 |
| **26** | (RR-Aib)$_3$PK-c[(CH$_2$)$_2$CONH(CH$_2$)$_4$]$^{3,7}$ [EIQSK]GISN$_L$KN$_L$ | 6.4 ± 0.9 | 10.4 ± 3.2 | 5.2 ± 0.8 |
| **27** | RRRRRRRRR ($R_9$) | >25 | >25 | >25 |
| **28** | GRKKRRQRRRPPQ (Tat) | >25 | >25 | >25 |
| **29** (scrambled) | RRRRRRRRR KMGISSMVQPKII | >25 | >25 | >25 |
| **Edelfosine** | – | 9 ± 0.2 | 0.6 ± 0.1 | 1 ± 0.2 |
| **Miltefosine** | – | 47.6 ± 0.6 | 2 ± 0.1 | 19 ± 1.6 |

[a] $LC_{50}$ concentration is defined as that causing 50% of cell death in the population. Dead parasites were identified by their increased permeability to propidium iodide.
[b] Results are representative of three independent experiments each performed in triplicate.
[c] All the peptides are acylated and as carboxamides at the N-terminal and C-terminal end, respectively.

Remarkably, no significant leishmanicidal activity was observed upon incubation of the parasites with non-conjugated $R_9$ (**27**) and Tat (**28**) peptides. Similarly, conjugation of $R_9$ with a scrambled peptide with identical amino acid composition but different sequence than our prototype **1** (**29**) did not show any relevant leishmanicidal activity. Thus, it appears that neither the nature of the linker nor the linking position of the CPP (N- *vs* C-terminus) has a great impact on the potency of the compounds, and the same can be said about the linear or cyclic character of the target peptide conjugates. On the contrary, the sequence composition of the parent peptide in the conjugates is critical for activity.

Next, the ability of the CPP-conjugated compounds to enter the parasites was evaluated by fluorescence microscopy. Conjugate **30**, with a fluorescein moiety linked to the N-terminal position of linear prototype **1** (through a polymethylene spacer) and $R_9$ conjugated at the C-terminal end, was designed for these studies (Fig. S2, see Supplementary material). Remarkably, parasites exposed to **30** (Fig. 4) for a short 4-h period showed a localized green fluorescence near the flagellar pocket, a complex structure close to the flagellum that is responsible for most of the trafficking through the plasma membrane (Fig. 4A). To our knowledge, this is the first description of a basal localization of a CPP-conjugated compound in *Leishmania* promastigotes. 24 h after addition of the peptides the fluorescence extended to most of the cellular body (Fig. 4B). Both results demonstrate that $R_9$ conjugation allows cell penetration of our designed peptides and is essential for the observed cytotoxic activity against the parasites.

## 3. Conclusions

To improve both the stability against proteases and the leishmanicidal activity of linear prototype peptides targeting the dimer interface of Li-TryR, we decided to combine advantages derived from the introduction of side-chain crosslinks and the use of CPPs. A positional scanning study allowed us to define the optimal cyclization positions to preserve inhibition of Li-TryR activity and dimerization and 2- to 3-fold increase stability against proteinase K. The data presented here indicate that our designed lactam-bridged peptides are potent inhibitors of Li-TryR activity and dimerization when the side-chain crosslink is properly located in the 13-mers so as to allow some residual flexibility. Interestingly, we demonstrate, for the first time to the best of our knowledge, *in vitro* activity against *Leishmania infantum* resulting from the conjugation of peptide-based inhibitors of TryR dimerization with cationic CPPs. Furthermore, we were able to show precise internal localization of a fluorescent derivative near the structure of the flagellar pocket. All in all, these results support our initial hypothesis that disruption of the dimerization interface of TryR may be a useful strategy for the development of new drugs against this parasitic target.

## 4. Experimental section

### 4.1. Chemistry

#### 4.1.1. General methods

Unless otherwise noted, analytical grade solvents and commercially available reagents were used without further purification. DIEA, piperidine, $Ac_2O$, and EDT were purchased from *Aldrich* (Germany), TFA from Fluka (Germany) and HCTU from Fluorochem (UK). Fmoc-protected amino acids were purchased from Fluorochem (UK), *Polypeptide* (France), *Novabiochem* (Merck, Germany) and *Iris Biotech* (Germany). Fmoc-protected Rink Amide MBHA resin (0.56 mmoL/g and 0.38 mmoL/g loading) was purchased from *Iris Biotech* (Germany) and *Novabiochem*. [Fluorescein]-[PEG]-[peptide **1**] and [Fluorescein]-[PEG]-[peptide **3**] **20** and **21**, [CPPs]-[Peptide] conjugates **22**–**26** and **29**, CPPs sequences **27** and **28** and [Fluorescein]-[peptide **1**]-[$R_9$] **30** were purchased from Peptide Protein Research (UK) and Genosphere Biotechnologies (France). The pure products were analyzed by HPLC and electrospray ionization mass spectrometry (ESI-MS).

Lactam-bridged peptides **3**–**8** and linear precursors **14**–**19** were synthesized manually on a 20-positions manifold (*Omega*) in a 20-mL polypropylene syringe (*Dubelcco*) equipped with a porous polyethylene filter. The coupling reactions were carried out on solid phase using microwave radiation in a *Biotage Initiator* reactor in a 5-mL vial. Excluding the coupling reaction on the microwave reactor, the rest of the SPPS reactions were stirred using an *IKA-100* orbital shaker. After cleavage, the acidic crudes were sedimented in $Et_2O$ on a *Hettlich Universal* 320R centrifuge at 5000 rpm. All the crude and samples were lyophilized using mixtures water/acetonitrile on a Telstar 6–80 instrument. The monitoring of the reactions was also performed by HPLC/MS through a HPLC-waters 12695 connected to a Waters Micromass ZQ spectrometer. The linear peptides were purified on a *Biotage Isolera* instrument using reverse phase columns (KP-C18-HS 12 g) and the cyclic peptides were purified on a semipreparative HPLC instrument. As mobile phase, mixtures of A:B were used, where A = 0.05% TFA water and B = acetonitrile with a flow rate of 7 mL/min. The peptides were purified using a gradient from 0% of B to 100% of B in 30–45 min and were detected at 217 nm.

The purity of the peptides was checked by analytical RP-HPLC on an Agilent Infinity instrument equipped with a Diode Array and a C18 Sunfire column (4.6 mm × 150 mm, 3.5 μm). As mobile phase, A:B mixtures were used, where A = 0.05% TFA water and

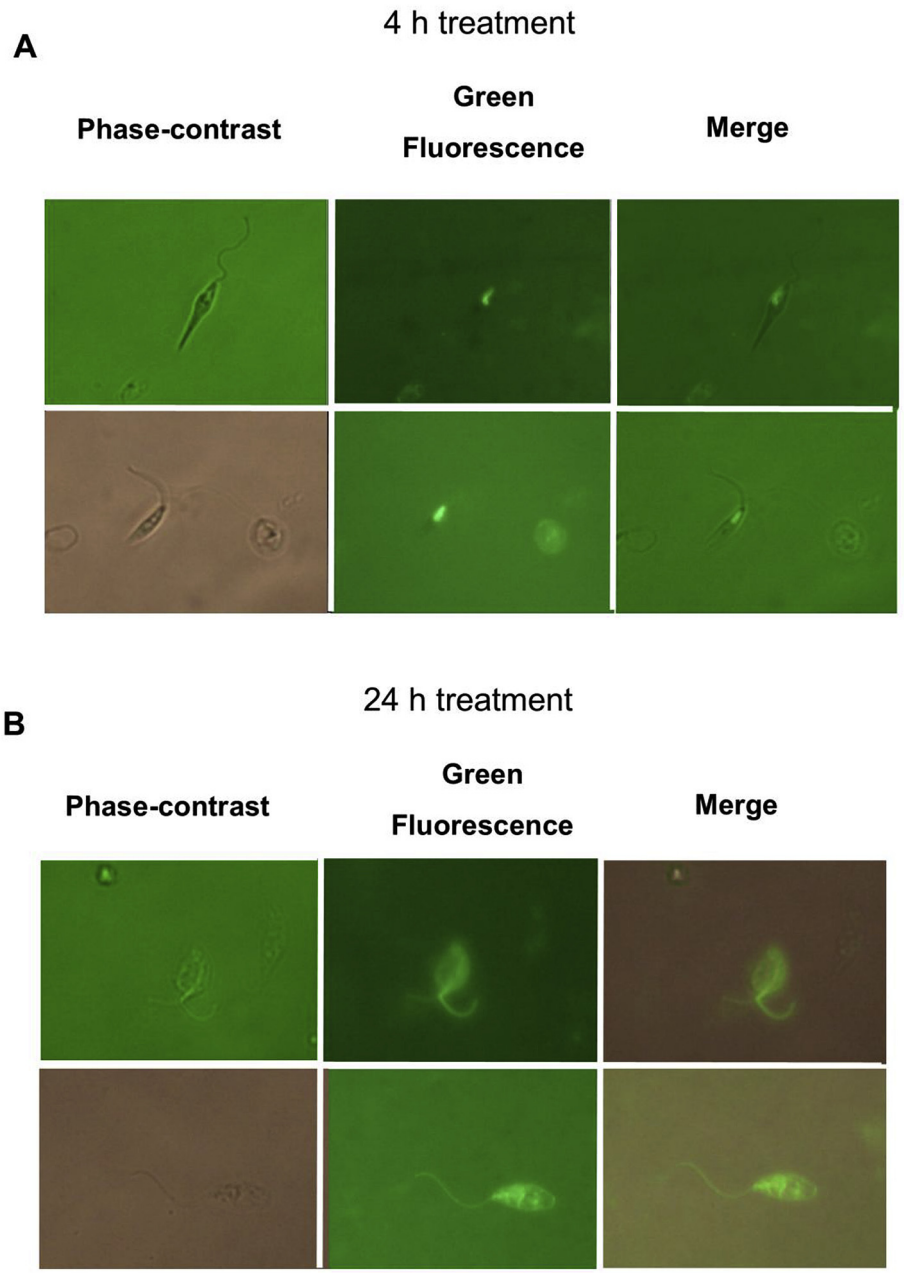


**Fig. 4.** Fluorescence microscopy images of *L. infantum* promastigotes incubated for 4 h (A) or 24 h (B) with a [fluorescein]-$(CH_2)_6$-[linear peptide **1**]-$[R_9]$ conjugate (**30**). Three different parasites are shown in each panel.

B = acetonitrile. The samples were analyzed at 214 and 254 nm in a gradient from 2% of B to 100% of B in 15 min (gradient 1). HRMS (EI+) was carried out in an Agilent 6520 Accurate-Mass Q-TOF LC/MS spectrometer using water/acetonitrile mixtures.

*4.1.2. Solid-phase peptide synthesis (SPPS)*

Cyclic peptides **3**–**8** and linear precursors **14**–**19** were synthesized manually on resin following the standard Fmoc/*t*Bu solid-phase orthogonal protection strategy.

*4.1.2.1. General coupling procedure.* Fmoc-protected Rink Amide MBHA resin was swollen in DCM/DMF/DCM/DMF (4 × 0.5 min). Then, the resin was treated with a mixture of DBU:piperidine:DMF (1:1:48, in volume) at room temperature (1 × 1 min) and (3 × 10 min) and washed with DMF/DCM/DMF/DCM (4 × 0.5 min). Later, to the free *Nα*-terminal swollen resin (1 equiv.), a solution of the corresponding Fmoc-AA-OH (1.2 equiv.), HCTU (1.2 equiv.) and DIEA (2.4 equiv.) in dry DMF (5 mL) was added. After sealing the vial, the reaction was heated in a microwave vial equipped with a magnetic stirrer for 10 min at 40 °C. Then, the vial was opened, the supernatant removed and new coupling mixture added. This process was repeated 3 times in total (3 × 10 min) until complete coupling. Finally, the resin was transferred to a fritted syringe, drained and washed extensively (DMF/DCM/DMF/DCM, 5 × 0.5 min). This protocol was repeated for the sequential anchoring of each amino acid. Coupling reactions to primary amines were monitored by the Kaiser ninhydrin test and to secondary amines by the Choranil test. In some cases, the progress of

the reactions was also followed by analysis of a small sample of peptidylresin after acidic cleavage in an HPLC-MS instrument.

*4.1.2.2. General acetylation procedure.* After elongation of the peptides, the *N*-terminal group was acetylated in all the cases by DBU deprotection of the Fmoc-resin-bounded derivative as mentioned above followed by treatment of the deprotected resin with a mixture of $Ac_2O$:DIEA:DMF (1:1:1, in volume) at room temperature (1 × 1 min) and (4 × 10 min). The resin was finally washed with DMF/DCM/DMF/DCM (4 × 0.5 min).

*4.1.2.3. Selective deprotection of allyl ester (OAl) and allyloxycarbonyl (Alloc) groups.* To the peptidyl resins swollen in anhydrous $CH_2Cl_2$ in a syringe, $Pd(PPh_3)_4$ (0.25 equiv.) and $PhSiH_3$ (24 equiv.) were added in anhydrous $CH_2Cl_2$ and the syringe was sealed and gently bubbled with argon. Then, the reaction was stirred at room temperature for 1 h. Then, the supernatant removed and new coupling mixture added for 1 h (2 × 1 h in total). The resin was then filtered and washed successively with $CH_2Cl_2$/DMF/$Et_2NCS_2Na$ 0.2 M in DMF/DMF/$CH_2Cl_2$ to remove residual palladium impurities.

*4.1.2.4. Selective deprotection of (PhiPr) and (Mmt) groups.* Deprotection was carried out using a mixture of TFA:TIPS:$H_2O$ 1:2:97 in 30 min. Then, the supernatant was removed and new deprotection mixture was added. This process was repeated twice in total (2 × 30 min).

*4.1.2.5. Amide-bridge cyclization.* After, acetylation of the peptides, the resin was swollen and treated with PyBOP (3 equiv.) and DIEA (6 equiv.) in NMP at room temperature for 1 h. Then, the resin was drained and washed extensively (DMF/DCM/DMF/DCM, 5 × 0.5 min).

*4.1.2.6. General cleavage procedure.* The well dried resin-bound derivative (1 vol) in a fritted syringe was treated with TFA:TIPS:$H_2O$ 95:2.5:2.5 (5 vol) for 4 h at room temperature. The filtrates were precipitated over cold $Et_2O$ and centrifuged three times at 5000 rpm for 10 min. After removing the supernatant, the pellet was redissolved in water/acetonitrile and lyophilized. The crudes were purified to give the target peptides in high purity.

*4.1.2.7. Ac-PK-c[$(CH_2)_2CONH(CH_2)_4$]$^{3,7}$[EIQSK]GIS$N_L$K$N_L$-$NH_2$ (**3**).* The general protocol was followed with 0.025 mmol of resin. After acetylation and deprotection of Glu and Lys side chains, cyclization was carried out with PyBOP and DIEA in NMP. The amide-cyclic peptide was cleaved and purified by reverse phase chromatography using semipreparative HPLC to give **3** as a white lyophilized cotton-like solid (3.71 mg, 12% overall yield).

HPLC (gradient 1): 6.64 min (98% analytical purity). HRMS (ESI,+) m/z: calculated for $C_{67}H_{118}N_{18}O_{18}$ 1462.8934; found 1462.8871 (−4.28 ppm).

*4.1.2.8. Ac-PKI-c[$(CH_2)_2CONH(CH_2)_4$]$^{4,8}$[EQSVK]IS$N_L$K$N_L$-$NH_2$ (**4**).* Starting from 0.114 mmol of resin, and after following the general protocol for elongation, acetylation, deprotection of side chains and cyclization, **4** was purified and isolated as a white lyophilized cotton-like solid (22.99 mg, 13% overall yield).

HPLC (gradient 1): 8.79 min (99% analytical purity). HRMS (ESI,+) m/z: calculated for $C_{70}H_{124}N_{18}O_{18}$ 1504.9352; found 1504.9341 (0.72 ppm).

*4.1.2.9. Ac-PKIIQS-c[$(CH_2)_2CONH(CH_2)_4$]$^{7,11}$EGISKK$N_L$-$NH_2$ (**5**).* The general protocol for elongation was followed with 0.095 mmol of resin. Once Fmoc-Glu-(O-2-PhiPr)-OH was introduced, selective deprotection of Glu and Lys side chains was carried out following the general protocol. After cyclization, elongation of the peptide was completed. Then, acetylation, cleavage and purification were performed to give **5** as a white lyophilized cotton-like solid (25.38 mg, 18% overall yield).

HPLC (gradient 1): 7.30 min (>99% analytical purity). HRMS (ESI,+) m/z: calculated for $C_{67}H_{118}N_{18}O_{18}$ 1462.8880; found 1462.8871 (0.61 ppm).

*4.1.2.10. Ac-PKIIQSV-c[$(CH_2)_2CONH(CH_2)_4$]$^{8,12}$[EIS-$N_L$-K]$N_L$-$NH_2$ (**6**).* From 0.342 mmol of resin and following the general protocols, 27 mg (9% overall yield) of **6** were obtained as a white lyophilized cotton-like solid.

HPLC (gradient 1): 10.72 min (97% analytical purity). HRMS (ESI,+) m/z: calculated for $C_{70}H_{123}N_{17}O_{18}$ 1489.9234; found 1489.9232 (0.14 ppm).

*4.1.2.11. Ac-PK-c[$(CH_2)_2CONH(CH_2)_4$]$^{3,7}$[EIQSK]GI-$NH_2$ (**7**).* From 0.084 mmol of resin and after elongation, acetylation, cyclization and purification **7** was isolated (13.72 mg, 16% overall yield) as a white cotton-like solid.

HPLC (gradient 1): 11.94 min (96% analytical purity). HRMS (ESI,+) m/z: calculated for $C_{46}H_{79}N_{13}O_{13}$ 1021.5936; found 1021.5920 (1.49 ppm).

*4.1.2.12. Ac-PKI-c[$(CH_2)_2CONH(CH_2)_4$]$^{4,8}$[EQSVK]I-$NH_2$ (**8**).* The general protocols were followed with 0.076 mmol of resin to give **8** as a white lyophilized cotton-like solid (19.52 mg, 24% overall yield).

HPLC (gradient 1): 6.13 min (95% analytical purity). HRMS (ESI,+) m/z: calculated for $C_{49}H_{85}N_{13}O_{13}$ 1063.6397; found 1063.6390 (0.66 ppm).

The synthesis of linear precursors **14**–**19** is detailed in the Supporting information.

## 5. Circular dichroism (CD)

CD spectra were recorded in a Jasco 715 (CIB, CSIC) over the 200–260 nm range at 25 °C in a 1 mm path-length cuvette. 4 scans were acquired for each sample (0.5–1.0 mg/mL in 30% TFE/water) and the mean spectra were finally considered. The presence of TFE as a helix promoting solvent was necessary to increase the aqueous solubility of peptides. Results were analyzed using the Spectrum Measurement software (Jasco, Easton, MD, USA).

## 6. Molecular dynamics (MD) simulations

Models for all linear and lactam-bridged peptides **1**–**8** were built using the Cartesian coordinates of the α-helix formed by residues Pro435-Met447 of monomer B of Li-TryR (PDB entry 2JK6) by introducing the covalent closure in the appropriate positions. In all cases, *N*- and *C*-terminal were defined as acetyl carbamate and carboxamide, respectively. All the systems were simulated in the same conditions as described previously [5]. Peptides **1**–**8** were introduced in a box of TIP3P waters using the tool *tleap*, integrated in the suite of programs AMBER 14.0 [31]. To do this, it was previously necessary to calculate the partial charges and force field parameters for the residues that participates in the lactam bridge: lysine (named as LYA) and glutamic acid (named as GLA). The cut-off distance for the nonbonded interactions was 12 Å and periodic boundary conditions were used. Electrostatic interactions were treated using the smooth particle mesh Ewald (PME) method with a grid spacing of 1 Å. The SHAKE algorithm was applied to all bonds involving hydrogen atoms and an integration step of 2.0 fs was used throughout. The system was progressively relaxed by energy minimizations, heated to 300K, and further simulated for a total time of 150 ns without any restraints, as described previously [9]. The

average degree of theoretical helicity per residue in 5–10 was assessed with the DSSP [32] algorithm along the course of 150-ns MD simulations at 300 K.

## 7. Protease susceptibility assays

Stock solutions of proteinase K were prepared in tris-buffered saline (TBS buffer) (50 μg/mL based on weight to volume). Stock solutions of the linear peptide **1** and the amide-bridge cyclic analogues **3** and **4** (100 μM) were prepared using 10% DMSO in TBS buffer (pH = 7.6, Aldrich). For the proteolysis reaction, the former peptide stock solutions (200 μL) were mixed with TBS (120 μL). Then, proteinase K stock solution (80 μL) was added (final concentration enzyme 10 μg/mL), the solution mixed, and finally allowed to proceed at room temperature with orbital shaking. Then, the enzymatic reaction was quenched (50 μL) at the desired time point (0, 5, 15, 30, 60, 180 and 360 min for linear peptide **1** and 0, 15, 30, 60, 120, 240, 360, 480, 540 min and 24 h for cyclic analogues **3** and **4** by addition of 1% TFA in water/acetonitrile 1:1 (100 μL). 100 μL of the resulting quenched reaction was injected onto an HPLC, and the amount of starting peptide present was quantified by integration of the peak at 214 nm. Triplicate reactions were run for each time point reported and half-lives were determined by fitting time dependent peptide concentration to an exponential decay using GraphPad Prism.

## 8. Li-TryR oxidoreductase activity

Oxidoreductase activity was determined according to the method described by Hamilton et al. [24]. Briefly, reactions were carried out at 26 °C (250 μL) of HEPES pH 8.0 (40 mM) buffer containing EDTA (1 mM), NADPH (150 μM), NADP+ (30 μM), DTNB (25 μM), T[S]2 (1 μM), glicerol (0.02%), DMSO (1.5%) and recombinant Li-TryR (7 nM). For $IC_{50}$ determinations (**1**–**8** and **14**–**19**) the enzyme was pre-incubated with the peptides (concentrations ranging from 75 μM to 0.29 μM) for 10 min prior the addition of T $[S]_2$ and NADPH. Enzyme activity was monitored by the increase in absorbance at 412 nm for 1 h at 26 °C in a VERSAmax microplate reader (Molecular Devices, California, USA). All the assays were conducted in triplicate in at least three independent experiments. Data were analyzed using a non-linear regression model with the Grafit6 software (Erithacus, Horley, Surrey, UK).

## 9. Dimer quantitation assay

The stability of the Li-TryR dimeric form in the presence of cyclic peptides **3**–**8** and linear prototypes **1** and **2** was evaluated using the novel Enzyme-Linked ImmunoSorbent Assay (ELISA) recently developed in our laboratory [9]. Briefly a dual (HIS/FLAG) tagged Li-TryR (400 nM) was incubated in a dimerization buffer (200 μL 300 mM NaCl, 50 mM Tris pH 8.0) for 16 h at 37 °C with agitation and in a humid atmosphere in the presence of different peptide concentration (10–90 μM). Next the plates were washed ten times with TTBS (Tween 0.1%, 2 mM Tris, 138 mM NaCl 138 pH 7.6) and incubated with diluted monoclonal α-HIS HRP conjugated antibody (200 μL, Abcam, Cambridge, UK) in BSA (5%) in TTBS for 1 h at room temperature. The plates were washed once again as previously described and 1,2-phenylenediamine dihydrochloride (OPD) substrate (100 μL, Dako, Glostrup, Denmark) prepared according to manufacturer's instructions was added. The enzymatic reaction was stopped after 10 min with $H_2SO_4$ (100 μL, 0.5 M) and the absorbances were measured at 490 nm in a VERSAmax microplate reader (Molecular Devices, California, USA). All the assays were conducted in triplicate in at least three independent experiments. Data were analyzed using a non-linear regression model with the Grafit6 software (Erithacus, Horley, Surrey, UK).

## 10. Cells and culture conditions

*L. infantum* axenic amastigotes were grown in M199 (Invitrogen, Leiden, The Netherlands) medium supplemented with 10% heat inactivated FCS, 1 g/L β-alanine, 100 mg/L L-asparagine, 200 mg/L sacarose, 50 mg/L sodium pyruvate, 320 mg/L malic acid, 40 mg/L fumaric acid, 70 mg/L succinic acid, 200 mg/L α-ketoglutaric acid, 300 mg/L citric acid, 1.1 g/L sodium bicarbonate, 5 g/L MES, 0.4 mg/L hemin, 10 mg/L gentamicine pH 5.4 at 37 °C. THP-1 cells were grown in RPMI-1640 medium (Gibco, Leiden, The Netherlands) supplemented with 10% heat inactivated FCS, antibiotics, 1 mM HEPES, 2 mM glutamine and 1 mM sodium pyruvate, pH 7.2 at 37 °C and 5% $CO_2$.

*L. infantum* promastigotes (MCAN/ES/89/IPZ229/1/89) were grown in RPMI-1640 medium (Sigma–Aldrich, St. Louis, MO, USA) supplemented with 10% heat-inactivated fetal calf serum (FCS), antibiotics, and 25 mm HEPES (pH 7.2) at 26 °C.

## 11. Leishmanicidal activity and cytotoxicity assays

Drug treatment of amastigotes was performed during the logarithmic growth phase at a concentration of $1 \times 10^6$ parasites/mL at 37 °C for 24 h. Drug treatment of promastigotes was performed during the logarithmic growth phase at a concentration of $2 \times 10^6$ parasites/mL at 26 °C for 24 h. Drug treatment of THP-1 cells was performed during the logarithmic growth phase at a concentration of $4 \times 10^5$ cells/mL at 37 °C and 5% $CO_2$ for 24 h. $LC_{50}$ was evaluated by flow cytometry by the propidium iodide (PI) exclusion method [33]. After selection of the parasite population based on their forward scatter (FSC) and side scatter (SSC) values, live and dead parasite cells were identified by their permeability to PI. This is a conservative procedure that may underestimate $LC_{50}$ values as parasites that became fragmented as a consequence of cell death are excluded from the analysis. To minimize the presence of fragmented parasites drug treatment never exceeded 24 h.

## Acknowledgements

We thank the Spanish Government (MINECO/FEDER Projects SAF2012-39760-C02 and SAF2015-64629-C2) and Comunidad de Madrid (BIPEDD-2-CM ref. S-2010/BMD-2457) for financial support.

## Appendix A. Supplementary data

Supplementary data related to this article can be found at http://dx.doi.org/10.1016/j.ejmech.2017.04.020.

## References

[1] Leishmaniasis, Fact Sheet N°375, February 2015. Available at: http://www.who.int/leishmaniasis/en/.
[2] Joo Hwan, No. visceral leishmaniasis: revisiting current treatments and approaches for future discoveries, Acta Trop. 155 (2016) 113–123.
[3] K. Shahnawaz, K. Irfan, P.M.S. Chauhan, Antileishmanial chemotherapy: present status and future perspectives, Chem. Biol. Interface 5 (2015) 1–28.
[4] J.N. Sangshetti, F.A. Kalam Khan, A.A. Kulkarni, R. Arote, R.H. Patil, Antileishmanial drug discovery: comprehensive review of the last 10 years, RSC Adv. 5 (2015) 32376–32415.
[5] (For a review see) a) V. Olin-Sandoval, R. Moreno-Sánchez, E. Saavedra, Targeting trypanothione metabolism in trypanosomatid human parasites, Curr. Drug Targets 11 (2010) 1614–1630;
b) A.E. Leroux, R.L. Krauth-Siegel, Thiol redox biology of trypanosomatids and potential targets for chemotherapy, Mol. Biochem. Parasitol. 206 (2016) 67–74.
[6] a) R.H. Schirmer, J.G. Müller, R.L. Krauth-Siegel, Disulfide-reductase inhibitors as chemotherapeutic agents: the design of drugs for trypanosomiasis and

malaria, Angew. Chem. Int. Ed. 34 (1995) 141–154;
b) R.L. Krauth-Siegel, H. Bauer, R.H. Schirmer, Dithiol proteins as guardians of the intracelular redox milieu in parasites: old and new drug targets in trypanosomes and malaria-causing plasmodia, Angew. Chem. Int. Ed. 44 (2005) 690–715.

[7] a) M.O.F. Khan, Trypanothione reductase: a viable chemotherapeutic target for antitrypanosomal and antileishmanial drug design, Drug Target Insights 2 (2007) 129–146;
b) L.S.C. Bernardes, C.L. Zani, I. Carvalho, Trypanosomatidae diseases: from the current therapy to the efficacious role of trypanothione reductase in drug discovery, Curr. Med. Chem. 20 (2013) 2673–2696.

[8] G. Colotti, P. Baiocco, A. Fiorillo, A. Boffi, E. Poser, F. Di Chiaro, A. Llari, Structural insights into the enzymes of the trypanothione pathway: targets for antileishmaniasis drugs, Future Med. Chem. 15 (2013) 1861–1875.

[9] M.A. Toro, P.A. Sánchez-Murcia, D. Moreno, M. Ruiz-Santaquiteria, J.F. Alzate, A. Negri, M.J. Camarasa, F. Gago, S. Velázquez, A. Jiménez-Ruiz, Probing the dimerization interface of Leishmania infantum trypanothione reductase with site-directed mutagenesis and short peptides, ChemBioChem 14 (2013) 1212–1217.

[10] P.A. Sánchez-Murcia, M. Ruiz-Santaquiteria, M.A. Toro, H. De Lucio, M.A. Jiménez, F. Gago, A. Jiménez-Ruiz, M.J. Camarasa, S. Velázquez, Comparison of hydrocarbon- and lactam- bridged cyclic peptides as dimerization inhibitors of of Leishmania infantum trypanothione reductase, RSC Adv. 5 (2015) 55784–55794.

[11] See for example N.E. Shepherd, H.N. Hoang, V.S. Desai, E. Letouze, P.R. Young, D.P. Fairlie, Modular α-helical mimetics with antiviral activity against respiratory syncytial virus, J. Am. Chem. Soc. 128 (2006) 13284–13289.

[12] M.I. García-Aranda, Y. Mirassou, B. Gautier, M. Martín-Martínez, N. Inguimbert, M. Vidal, M.T. García-López, M.A. Jiménez, R. González-Muñiz, M.J. Pérez de Vega, Disulfide and amide-bridged cyclic peptide analogues of the VEGF(81-91) fragment: synthesis, conformational analysis and biological evaluation, Bioorg. Med. Chem. 19 (2011) 7526–7533.

[13] K.K. Khoo, M.J. Wilson, B.J. Smith, M.-M. Zhang, J. Gulyas, D. Yoshikami, J.E. Rivier, G. Bulaj, R.S. Norton, Lactam-stabilized helical analogues of the analgesic μ-conotoxin KIIIA, J. Med. Chem. 54 (2011) 7558–7566.

[14] M.I. García-Aranda, S. González-López, C.M. Santiveri, N. Gagey-Eilstein, M. Reille-Seroussi, M. Martín-Martínez, N. Inguimbert, M. Vidal, M.T. García-López, M.A. Jiménez, R. González-Muñiz, M.J. Pérez de Vega, Helical peptides from VEGF and Vammin hotspots for modulating the VEGF–VEGFR interaction, Org. Biomol. Chem. 11 (2013) 1896–1905.

[15] See for example recent reviews P.M. Cromm, J. Spiegel, T.N. Grossmann, Hydrocarbon stapled peptides as modulators of biological function, ACS Chem. Biol. 10 (2015) 1362–1375.

[16] See also L.D. Walensky, G.H. Bird, Hydrocarbon-stapled peptides: principles, practice, and progress, J. Med. Chem. 57 (2014) 6275–6288.

[17] For reviews on covalent cyclization approach see for example ref. 17-19 C.J. White, A.K. Yudin, Contemporary strategies for peptide macrocyclization, Nat. Chem. 3 (2011) 509–524.

[18] Y.H. Lau, P. de Andrade, Y. Wu, D.R. Spring, Peptide stapling techniques based on different macrocyclisation chemistries, Chem. Soc. Rev. 44 (2015) 91–102.

[19] T.A. Hill, N.E. Shepherd, F. Diness, D.P. Fairlie, Constraining cyclic peptides to mimic protein structure motifs, Angew. Chem. Int. Ed. 53 (2014) 13020–13041.

[20] J. Zhu, R.E. Marchant, Solid-phase synthesis of tailed cyclic RGD peptides using glutamic acid: unexpected glutarimide formation, J. Pept. Sci. 14 (2008) 690–696.

[21] P. Luo, R.L. Baldwin, Mechanism of helix induction by Trifluoroethanol: a framework for extrapolating the helix-forming properties of peptides from trifluoroethanol/water mixtures back to wate, Biochemistry 36 (1997) 8413–8421.

[22] D. Roccatano, G. Colombo, M. Fioroni, A.E. Mark, Mechanism by which 2,2,2-trifluoroethanol/water mixtures stabilize secondary-structure formation in peptides: a molecular dynamics study, Proc. Natl. Acad. Sci. U. S. A. 99 (2002) 12179–12184.

[23] M. Buck, Trifluoroethanol and colleagues: cosolvents come of age. Recent studies with peptides and proteins, Q. Rev. Biophys. 31 (1998) 297–355.

[24] C.J. Hamilton, A. Saravanamuthu, I.M. Eggleston, A.H. Fairlamb, Ellman's-reagent-mediated regeneration of trypanothione in situ: substrate-economical microplate and time-dependent inhibition assays for trypanothione reductase, Biochem. J. 369 (2003) 529–537.

[25] Some example of recent reviews ref. 25-27 J.D. Ramsey, N.H. Flynn, Cell-penetrating peptides transport therapeutics into cells, Pharmacol. Ther. 154 (2015) 78–86.

[26] D.A. Copolovici, K. Langel, E. Eriste, Ü. Langel, Cell-penetrating peptides: design, synthesis, and applications, ACS Nano 8 (2014) 1972–1994.

[27] C. Bechara, S. Sagan, Cell-penetrating peptides: 20 years later, where do we stand? FEBS Lett. 587 (2013) 1693–1702.

[28] J.R. Luque-Ortega, B.G. de la Torre, V. Hornillos, J.M. Bart, C. Rueda, M. Navarro, F. Amat-Guerri, A.U. Acuña, D. Andreu, L. Rivas, Defeating Leishmania resistance to miltefosine (hexadecylphosphocholine) by peptide-mediated drug smuggling: a proof of mechanism for trypanosomatid chemotherapy, J. Control. Release 161 (2012) 835–842.

[29] M.A. Abengózar, J.R. Luque-Ortega, V. Hornillos, et al., Congreso II GEQB/XIV EPI, Bilbao (2013) P53.

[30] H. Yamashita, Y. Demizy, T. Shoda, Y. Sato, M. Oba, M. Tanaka, M. Kurihara, Amphipathic short helix-stabilized peptides with cell-membrane penetrating ability, Bioorg. Med. Chem. 22 (2014) 2403–2408.

[31] D.A. Case, R.M. Betz, W. Botello-Smith, D.S. Cerutti, T.E. Cheatham III, T.A. Darden, R.E. Duke, T.J. Giese, H. Gohlke, A.W. Goetz, N. Homeyer, S. Izadi, P. Janowski, J. Kaus, A. Kovalenko, T.S. Lee, S. LeGrand, P. Li, C. Lin, T. Luchko, R. Luo, B. Madej, D. Mermelstein, K.M. Merz, G. Monard, H. Nguyen, H.T. Nguyen, I. Omelyan, A. Onufriev, D.R. Roe, A. Roitberg, C. Sagui, C.L. Simmerling, J. Swails, R.C. Walker, J. Wang, R.M. Wolf, X. Wu, L. Xiao, D.M. York, P.A. Kollman, AMBER, University of California, San Francisco, 2016.

[32] J. Klett, A. Núñez-Salgado, H.G. Dos Santos, A. Cortés-Cabrera, A. Perona, R. Gil-Redondo, D. Abia, F. Gago, A. Morreale, Mm-ismsa: an ultrafast and accurate scoring function for protein–protein docking, J. Chem. Theory Comput. 8 (2012) 3395–3408.

[33] J.F. Alzate, A. Arias, F. Mollinedo, E. Rico, J. de la Iglesia-Vicente, A. Jimenez-Ruiz, Edelfosine induces an apoptotic process in Leishmania infantum that is regulated by the ectopic expression of Bcl-XL and Hrk, Antimicrob. Agents Chemother. 52 (2008) 3779–3792.